Two additional measurements were made from the R.V. *Alcoa Seaprobe* by using a drill rig equipped with a 2000-m drill pipe, television camera pod, and hook apparatus, at a station 32 km southwest of the bottom station and at the same depth (39°44′N, 70°57′W). A total of ten measurements of total oxygen uptake and two measurements of chemical oxygen demand were made during June and August 1972. We calculated oxygen uptake rates from the slopes of the recorder graphs, visual records of bell jar penetration depth, and the oxygen concentration of the bottom water (7.15 ml of O_2 per liter at 4.5°C).

Oxygen uptake under the bell jars ranged from 0.39 to 0.55 ml m^{-2} hr^{-1} at the bottom station. Both values at the other station were 0.62 ml m^{-2} hr^{-1}. The difference between the two sites is statistically significant ($P < .05$), but the mean of all ten values, 0.50 ± 0.03, is two orders of magnitude lower than the values from shallow depths (Table 1). We detected no residual oxygen uptake after the addition of Formalin, which indicates that more than 99 percent of the uptake was due to biological activity. This suggests that the accumulation of biologically oxidizable organic matter is negligible. If it were not, we would expect the sediments to become anoxic and accumulate reduced compounds (*8*). The lack of organic accumulation supports the general belief that food is limiting to deep-sea communities.

Pamatmat (*4*) made measurements between 2750 and 2900 m off the coasts of Peru and Washington. His values are an order of magnitude larger than ours (1.5 to 4.5 ml m^{-2} hr^{-1}) with a reported chemical oxygen uptake of 66 to 106 percent of the total. Part of this high value may be due to decompression during retrieval of the cores and higher experimental temperatures. But surface production is high in these regions of the Pacific coast (upwelling regions), and a part of the high uptake is undoubtedly due to a greater food supply at the bottom. This explanation is supported by the high chemical uptake found.

We do not have samples or measurements of the animal biomass under our bell jars. However, measurements by Rowe *et al.* (*9*) at the same bottom site indicate a decrease of one order of magnitude in biomass between shelf depths (30 to 100 m) and the deep site. Since the decrease in oxygen uptake between shelf and deep slope in the western Atlantic is two orders of magnitude (Table 1), we might conclude that the deep benthic animals are less active metabolically than their shallower living relatives. However, in shallow benthic systems, bacterial metabolism accounts for most of the oxgen uptake (*10*). If this is also true at 1850 m, the decrease with depth can be accounted for by the decrease in bacterial metabolism. We think our community respiration measurements are more typical for deep slope depths than those of Pamatmat (*4*) and that oxygen consumption is even lower at greater depths. Hence, the metabolic activity of deep-sea benthic communities, which occupy more than 76 percent of the world's ocean bottom (*11*), is low.

K. L. Smith, Jr., J. M. Teal
Woods Hole Oceanographic Institution, Woods Hole, Massachusetts 02543

References and Notes

1. G. T. Rowe, *Fertility of the Sea*, J. Costlow, Ed. (Gordon & Breach, New York, 1971), vol. 2.
2. H. L. Sanders, R. R. Hessler, G. R. Hampson, *Deep-Sea Res.* **12**, 845 (1965).
3. H. W. Jannasch, K. Eimhjellen, C. O. Wirsen, A. Farmanfarmian, *Science* **171**, 672 (1971).
4. M. M. Pamatmat, *Limnol. Oceanogr.* **16**, 536 (1971).
5. B. Ya. Vilenkin, *Dokl. Akad. Nauk SSSR Oceanol. Sect.* **5**, 128 (1965).
6. The currents and temperatures at the bottom were measured by members of the Biology Department of Woods Hole Oceanographic Institution working at the deep station.
7. J. Kanwisher, *Limnol. Oceanogr.* **4**, 210 (1959).
8. J. M. Teal and J. Kanwisher, *ibid.* **6**, 388 (1961).
9. G. T. Rowe, P. T. Polloni, S. G. Hornor, unpublished manuscript.
10. J. Kanwisher, *Occas. Publ. Grad. Sch. Oceanogr. Univ. R.I.* **1**, 13 (1962); K. L. Smith, Jr., thesis, University of Georgia (1971); ———, G. T. Rowe, J. Nichols, *J. Coast. Mar. Sci.*, in press.
11. A. F. Brunn, *Treatise on Marine Ecology and Paleoecology*, J. W. Hedgpeth, Ed. (Geological Society of America, Washington, D.C., 1957), vol. 1, p. 641.
12. K. L. Smith, Jr., K. A. Burns, J. M. Teal, *Mar. Biol.* **12**, 196 (1972).
13. Contribution No. 2957 from the Woods Hole Oceanographic Institution. Supported by ONR contract 241. We thank the D.S.R.V. *Alvin* group and the crew of the R.V. *Lulu* for assistance and H. Jannasch, H. Sanders, G. Rowe, F. Grassle, R. Backus, P. Wiebe, and C. Wirsen for critically reading the manuscript.

5 October 1972

Convergent Projection of Three Separate Thalamic Nuclei on to a Single Cortical Area

Abstract. *Three distinct sensory-motor nuclei in the thalamus project to parietal cortex in the Virginia opossum; the ventral posterior nucleus receives inputs from somatic sensory structures and projects to layers IV and III, the ventral anterolateral nucleus receives inputs from motor structures and projects to layers IV and III and inner I, and the central intralaminar nucleus receives inputs from sensory, motor, and other structures and projects to layers VI through outer I. The physiologically defined amalgamation of somatic sensory and motor cortex is correlated, therefore, with the extent of cortex that receives convergent somatic sensory and motor input from the thalamus.*

Since Morison and Dempsey first provided electrophysiological evidence of more than one thalamic influence on each area of the cortex (*1*), neurophysiologists have accumulated further support for this concept (*2*). However, anatomical evidence has not provided clear or consistent support for more than one thalamic projection to each cortical area. We have studied the somatic sensory-motor cortex of the opossum—an area extremely rich in convergent thalamic inputs (*3*)—in order to specify the total number of thalamic inputs and the distribution of their axonal terminals in each cortical layer.

In the opossum two divisions of the ventral thalamic nucleus which receive nonconvergent afferent fibers from either sensory or motor structures have been described (*4*). Projections from spinal, dorsal column, and trigeminal lemnisci to the thalamus were studied to identify the region that receives inputs from somatic sensory relay nuclei. Projections from cerebellum to the thalamus were studied to identify the equivalent thalamic nucleus to those cells that project to motor cortex in other mammals. The results showed that cells in the posterior two-thirds of the ventral nucleus receive fibers from somatic sensory relay nuclei, while those in the rostral one-third receive cerebellar fibers; there was no detectable overlap in the projection field of these fiber systems. In contrast, fibers from all of the afferent sensory and motor systems, as well as from the ascending reticular formation converge on a thalamic cell group outside of the ventral nucleus; these thalamic cells constitute the somatic sensory-motor part of the intralaminar system of nuclei. Sensory and motor afferents to

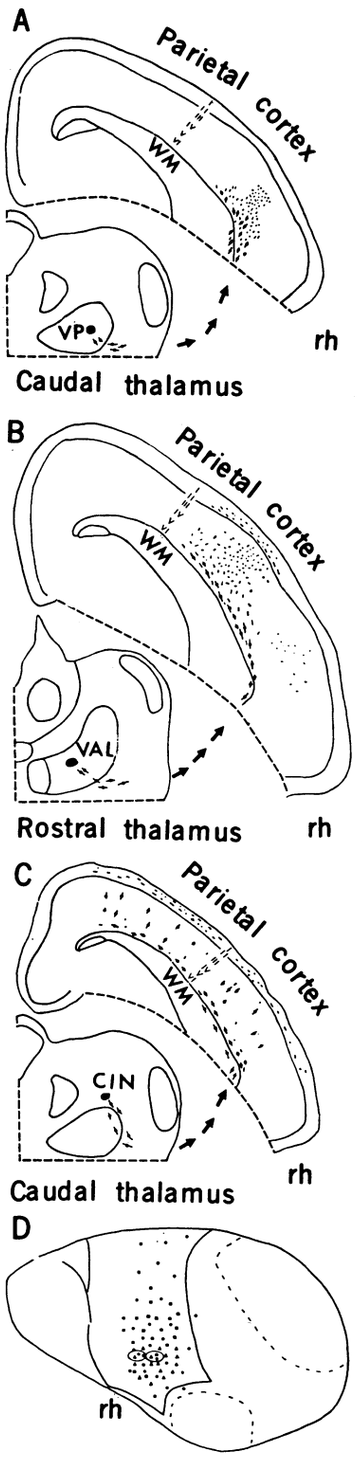

Fig. 1. Diagrams of transverse sections through thalamus and cortex to show the differences in the distribution of degenerated fibers after lesions of (A) *VP*, (B) *VAL*, and (C) *CIN*. Black areas in the thalamus indicate the extent of the lesion in a section through its maximum extent. Beaded lines show the course of degenerated fibers as they leave the area of the lesion and as they enter cortex; short lines and dots in cortex represent areas of fine fibers and terminals. Roman numerals indicate cortical layers. *WM*, cortical white matter; *rh*, rhinal fissure. (D) Surface view of opossum cerebral hemisphere showing the extent of parietal cortex (solid line), and within it the projection fields in the cases illustrated in (A), (B), and (C); VP, ▲; VAL, ■; CIN, ●. Ellipses enclose a cortical area containing all three overlapping projections in these cases.

the thalamus thus define three separate groups of thalamic cells that may project directly to opossum cortex: (i), the lemniscal input zone (ventral posterior nucleus or VP); (ii), the cerebellar input zone (ventral anterolateral nucleus or VAL); and (iii), the convergent somatic sensory, cerebellar, reticular formation input zone (central intralaminar nucleus or CIN).

The projection of each of these thalamic nuclei onto cortex was studied in the Virginia opossum by making punctate thalamic lesions with d-c current passed through the tip of a microelectrode. Six to seven days after the operation the animals were perfused with saline and then with 10 percent Formalin. The brains were excised and sectioned on a freezing microtome and stained with the Fink-Heimer technique for degenerated axons and axon terminals (*5*). Cases analyzed include 16 lesions restricted to VP, 8 lesions restricted to VAL, and 5 lesions restricted to CIN. Additional cases that contained lesions adjacent to these nuclei were analyzed, but no other thalamic cells were found that project to parietal cortex.

Thalamic nuclei that receive either convergent or nonconvergent afferent fibers from somatic sensory-motor structures project directly to parietal cortex. The VP, VAL, and CIN nuclei project to the same area, but to different combinations of cortical layers. Axons of VP cells are large-caliber fibers that arborize in layer V and terminate densely in layers IV and III of a restricted zone of parietal cortex (Fig. 1A). There is considerable topographic localization in this fiber system, but when the projection field from all cases were added together they include all of parietal cortex. Axons of VAL cells are medium- to large-caliber fibers that terminate in layers IV and III and in layer I in a restricted part of parietal cortex (Fig. 1B). The VAL fibers are relatively large caliber fibers compared to other fibers in layer I; they are located predominantly in the inner part of layer I, and they are found only above (superficial to) the dense layer IV and III terminal field (that is, they show a limited spread in layer I). The VAL fibers project with definite topographic localization; reconstruction of the total projection area, however, shows that it also includes all of parietal cortex. The terminal field of VAL fibers thus overlaps with that of VP fibers. Axons of CIN cells are fine caliber fibers, many of which give off collaterals in the putamen on their way to cortex. These fibers travel for long distances in the white matter under parietal cortex, branch repeatedly, and terminate in layers VI through I (Fig. 1C). The CIN fiber system shows relatively little topographic localization; even small lesions in CIN project to nearly all of parietal cortex without concentrated axon terminals in any part of the projection field. These projections thus overlap in their distribution with those of VP and VAL. The relative extent of projections of these three fiber systems, from lesions of nearly equal size, is illustrated in Fig. 1D.

Our conclusion from these studies is that three nuclei can be identified in the opossum thalamus that converge on a single area of cortex. The nuclei can be distinguished by their cytoarchitec-

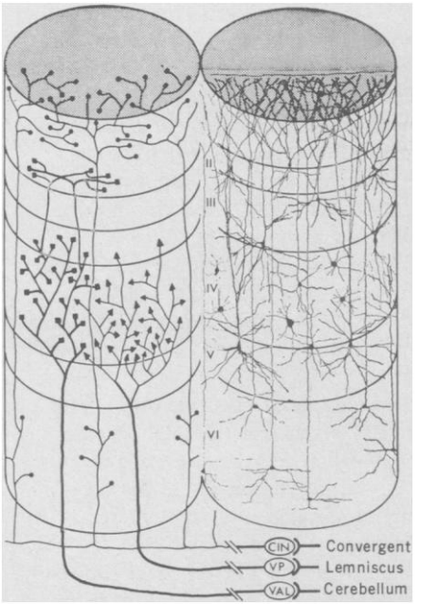

Fig. 2. Summary diagram of the three overlapping distribution patterns of thalamic fibers found in opossum parietal cortex. The VP, VAL, and CIN fiber patterns, as reconstructed from the distribution of degenerated fibers and terminals, are shown in the left cylinder. They can be compared with the cell bodies and dendrites that are present in each layer (right cylinder) as reconstructed from Golgi-Cox stained preparations [adapted from Walsh and Ebner (*9*)]. Detailed electron microscopic analysis would be required to specify the exact postsynaptic structures of each fiber system.

tural location and by their characteristic combinations of somatic sensory and motor inputs. All three nuclei project in a spatially overlapping manner to parietal cortex and terminate in the cortical layers as summarized in Fig. 2. This arrangement of somatic sensory and motor thalamocortical fiber systems in the marsupial opossum stands in contrast to that reported for placental mammals with the use of comparable techniques; for example, in the cat, the ventral posterior nucleus projects to layers IV and III of postcruciate cortex, while VL projects only to precruciate cortex (*6*). These anatomical species differences were predicted by parallel differences in physiological mapping results in the opossum and cat (*3*, *7*). In the opossum, the convergent projections from separate sensory and motor thalamic nuclei onto a single cortical area comprise an adequate anatomical correlate for a functionally amalgamated sensory-motor area.

The identification of three separate thalamic inputs to sensory cortex is not unique to the somatic sensory system of the opossum, since more than one input has already been reported for opossum visual cortex and hedgehog visual, auditory, and somatic sensory cortices (*8*). In sensory systems of both species, the results demonstrate that more than one thalamic influence is operating directly on each "column" of sensory cortex. Multiple thalamic inputs that terminate in different combinations of cortical layers provide a probable anatomical substrate for the variety of responses evoked in cortex after stimulation of different thalamic nuclei. For example, the restricted VP projection provides a reasonable substrate for the primary evoked response while the diffuse CIN projection may well underlie the recruiting response first discovered by Morison and Dempsey (*1*). However, further studies which combine anatomical and physiological techniques are necessary in order to more closely correlate physiological responses with their anatomical substrate.

H. KILLACKEY
F. EBNER

Section of Neurosciences, Division of Biological and Medical Sciences, Brown University, Providence, Rhode Island 02912

References and Notes

1. R. Morison and E. O. Dempsey, *Amer. J. Physiol.* **135**, 281 (1942).
2. O. Creutzfeldt, H. Lux, S. Watanabe, in *The Thalamus*, D. Purpura and M. Yahr, Eds. (Columbia Univ. Press, New York, 1966); C. L. Li, C. Cullen, H. Jasper, *J. Neurophysiol.* **19**, 111, 131 (1956).
3. R. Lende, *Science* **141**, 730 (1963).
4. T. Walsh and F. Ebner, *J. Comp. Neurol.*, in press.
5. R. Fink and L. Heimer, *Brain Res.* **4**, 369 (1967).
6. P. Hand and A. Morrison, *Exp. Neurol.* **26**, 291 (1970); E. Jones and T. Powell, *Brain Res.* **13**, 298 (1969); P. Strick, *ibid.* **20**, 130 (1970).
7. C. Woolsey, in *Biological and Biochemical Basis of Behavior*, H. Harlow and C. Woolsey, Eds. (Univ. of Wisconsin Press, Madison, 1958).
8. L. Benevento and F. Ebner, *J. Comp. Neurol.* **143**, 242 (1971); W. Hall, *Anat. Rec.* **166**, 313 (1970); H. Killackey, *ibid.* **172**, 345 (1972); ——— and F. Ebner, *Brain Behav. Evol.*, in press; R. Ravizza and I. T. Diamond, *Anat. Rec.* **172**, 390 (1972).
9. T. Walsh and R. Ebner, *J. Anat.* **107**, 1 (1970).
10. Supported by NINDS grant NS-06551 and fellowship NS-50714 (to H.P.K.). We thank E. W. Swick and E. DiPalma for assistance.

15 June 1972

Three-Dimensional Structure of Yeast Phenylalanine Transfer RNA: Folding of the Polynucleotide Chain

Abstract. *At 4 Å resolution the polynucleotides in yeast phenylalanine transfer RNA are seen in a series of electron dense masses about 5.8 Å apart. These peaks are probably associated with the phosphate groups, while lower levels of electron density between segments of adjacent polynucleotide chains are interpreted as arising from hydrogen-bonded purine-pyrimidine base pairs. It is possible to trace the entire polynucleotide chain with only two minor regions of ambiguity. The polynucleotide chain has a secondary structure consistent with the cloverleaf conformation; however, its folding is different from that proposed in any model. The molecule is made of two double-stranded helical regions oriented at right angles to each other in the shape of an* L. *One end of the* L *has the CCA acceptor; the anticodon loop is at the other end, and the dihydrouridine and TΨC loops form the corner.*

Transfer RNA (tRNA) has a key role in the translation of the polynucleotide sequences of messenger RNA into the polypeptide sequences of protein. A considerable body of information has accumulated regarding these molecules but up to the present time the three-dimensional folding of the polynucleotide chain was unknown. Eight years ago Holley and his collaborators sequenced alanine tRNA from yeast and pointed out that the sequence could be folded into a cloverleaf conformation in which there are four base paired stem regions connected with loops (*1*). Approximately 40 tRNA molecules from various sources have now been sequenced, and all of them can be arranged in a similar cloverleaf arrangement. We have been carrying out an x-ray diffraction analysis of yeast phenylalanine tRNA (*2*) whose sequence is known (*3*). Recently we described the heavy atom derivatives which allowed us to calculate a three-dimensional electron density map at 5.5 Å resolution (*4*). That map allowed us to discern the external shape of portions of the molecule and to trace short segments of the polynucleotide chain. We have continued this work and now report our interpretation of the electron density map at 4.0 Å resolution which allows us to determine the positions of most of the phosphate groups in the nucleotides of yeast phenylalanine tRNA. The polynucleotide chain has been traced and its three-dimensional folding is presented.

Yeast phenylalanine tRNA crystallizes in an orthorhombic unit cell, space group $P2_12_12_1$, $a = 33$ Å, $b = 56$ Å, and $c = 161$ Å, with four molecules in the unit cell (*2*). The methods used in preparing crystals of yeast phenylalanine tRNA, and the chemistry of the isomorphous heavy atom replacements have been described (*4*). Three types of heavy atom derivatives containing platinum, osmium, or samarium have been used. The 4 Å data including anomalous pairs were collected for the osmium and samarium derivatives and 5.5 Å data were collected for the platinum derivative. The positions of these heavy atoms have been reported (*4*). The overall figure of merit for the 2806 reflections collected is 0.70, and the R factors (modulus) are 0.58 for osmium 5.5 Å data; 1.56 for the 5.5 Å to 4.0 Å data; 0.47 for the 4.0 Å samarium data; and 1.05 for the 5.5 Å platinum data (*4*).

The electron density map reported at 5.5 Å resolution (*4*) had a number of intense peaks 5 to 7 Å apart, which were interpreted as arising from the phosphate groups of the tRNA polynucleotide chain. Although portions of the polynucleotide chain could be traced at 5.5 Å resolution, there were too many ambiguities to trace the entire chain. However, at 4.0 Å resolution the individual peaks of electron